

000 001 002 003 004 005 006 007 008 009 010 LANDMARK-GUIDED POLICY OPTIMIZATION FOR MULTI-OBJECTIVE LANGUAGE MODEL SELECTION

005 **Anonymous authors**

006 Paper under double-blind review

009 ABSTRACT

011 Selecting a pretrained large language model (LLM) to fine-tune for a task-specific
 012 dataset can be time-consuming and costly. With several candidate models avail-
 013 able to choose from, varying in size, architecture, and pretraining data, finding the
 014 best often involves extensive trial and error. In addition, the “best” model may
 015 not necessarily be the one with the lowest test loss, as practical considerations
 016 such as deployment costs, inference throughput, and limited search budgets might
 017 also play crucial roles. To address this, we introduce LAMPS (LAnguage Model
 018 Pareto Selection), a novel and open-source multi-objective AutoML framework
 019 that quickly identifies near-Pareto-optimal pretrained LLMs for a task-specific
 020 dataset. It is based on two key ideas: (1) landmark fine-tuning, which generates
 021 early performance indicators of the candidate models, and (2) meta-learning via
 022 reinforcement learning, which learns an effective selection policy from historical
 023 performance data (a meta-dataset). Our results show that, on held-out datasets,
 024 LAMPS reduces search time by an average of **73%71%** compared to exhaustive
 025 search, while still covering more than **99%98%** of the optimal target space hyper-
 026 volume.

027 1 INTRODUCTION

029 Fine-tuning a pretrained large language model (LLM) on task-specific datasets is currently the dom-
 030 inant paradigm for achieving state-of-the-art performance in several natural language processing
 031 (NLP) tasks (Radford et al., 2019), including question answering (Chowdhery et al., 2023), machine
 032 translation (Raffel et al., 2020), summarization (Aghajanyan et al., 2020), and classification (Yang,
 033 2019). However, different pretrained models yield varying downstream performance due to dif-
 034 ferences in size, architecture, pretraining data, and other intrinsic factors. Therefore, as the set of
 035 available pretrained models is already extensive, the important question arises: How can we effi-
 036 ciently find the best model for a task-specific dataset?

037 A common practice in NLP is to select the largest available model, driven by the belief that larger
 038 models invariably provide better performance (e.g., accuracy, F1, perplexity, cross-entropy, depend-
 039 ing on the downstream task). Although this is generally true, several studies have shown that smaller
 040 models are comparable to or even outperform larger ones for specialized tasks (Ouyang et al., 2022;
 041 Sanh et al., 2020; Hoffmann et al., 2022; Wahba et al., 2023; DeepSeek-AI et al., 2025; Wang et al.,
 042 2025). Moreover, in real-world scenarios, always choosing larger models inevitably leads to higher
 043 operational costs and greater environmental impact. This underscores the need to incorporate addi-
 044 tional factors into the model selection process beyond a single task-specific performance metric.

045 A multi-objective perspective is, then, essential to capture the broader spectrum of trade-offs that
 046 practitioners face when selecting pretrained LLMs for fine-tuning. In the absence of better alter-
 047 natives, practitioners may turn to exhaustive search. Although theoretically sound, this method
 048 quickly becomes prohibitively expensive for a large number of candidate models, especially for tar-
 049 get datasets with several million examples. As language models continue to expand in scale and
 050 diversity, there is an increasing need for a principled, holistic, and efficient selection strategy, es-
 051 pecially with the growing interest in specialized LLM-based AI agents (Gutowska, 2024; Ma et al.,
 052 2024).

053 In this paper, we introduce **LAMPS (LAnguage Model Pareto Selection)**, a novel and open-source
 054 multi-objective AutoML framework for selecting LLMs to fine-tune on task-specific datasets. It

integrates two complementary strategies: (1) *landmark fine-tuning*, which generates early performance indicators for candidate models by evaluating them on incrementally larger subsets of the training data; and (2) *meta-learning via reinforcement learning*, which leverages historical model performance data on multiple datasets to learn how to efficiently allocate training resources for new datasets. In other words, this process generates a policy that manages the selection and early stopping of candidate models, adjusting its strategy based on both observed and historical performance to efficiently discard low-potential models and prioritize promising ones.

Our main contributions are as follows: (i) Formulating the language model selection for fine-tuning explicitly as a multi-objective optimization problem; (ii) Introducing LAMPS, a novel and open-source AutoML framework combining landmark fine-tuning, meta-learning, and reinforcement learning to rapidly identify near-Pareto-optimal language models for a new task-specific dataset.

The remainder of the paper is organized as follows. Section 2 reviews relevant related work. Section 3 states the multi-objective optimization problem. The method is proposed in Section 5 and Section 6 presents the experimental setup and main findings. We conclude in Section 7.

2 RELATED WORK

Selecting an appropriate base learner (model, algorithm, pipeline, etc.) for a given task has been a long-standing research topic and is usually called *model selection* (Bozdogan, 1987; Maron & Moore, 1993; McQuarrie & Tsai, 1998; Chapelle et al., 2002; Biem, 2003; Brazdil et al., 2003; Zhao & Yu, 2006; Adankon & Cheriet, 2009). Among the different approaches available, meta-learning has been a popular choice (Kalousis & Hilario, 2000; Fürnkranz et al., 2002; Brazdil & Giraud-Carrier, 2018; Jain et al., 2024; de Amorim et al., 2025; Farhadi et al., 2025), mainly due to its ability to transfer knowledge from prior learning experiences, reducing the cost of exploration and improving sample efficiency.

In this section, we provide a brief overview of the related areas that form the foundation of our LAMPS framework.

Pretrained Model Selection in Deep Learning Fine-tuning pretrained deep learning models for specific downstream tasks has become the standard approach in both computer vision and natural language processing. Compared to training from scratch, fine-tuning is far more efficient and requires much less data than pretraining (Hepburn, 2018). For this reason, being able to select the right pretrained model efficiently is becoming increasingly relevant due to the considerable computational costs and the rapid introduction of new models with varying sizes, architectures, training data, and capabilities. To the best of our knowledge, the only work that explicitly addresses the selection of LLMs for fine-tuning is by Monteiro et al. (2024), but it neither considers the multi-objective aspects of the model selection nor adjusts its recommendations based on actual fine-tuning learning curves.

Subsampling Landmarks A sampling landmark is a performance-based meta-feature, representing the performance of a particular model on samples of available data, providing a quick estimate of its performance (Brazdil et al., 2022; Pfahringer et al., 2000) and, consequently, allowing indirect characterization of the target dataset. One variant is called *subampling landmarks*, which considers a sequence of sample sizes in increasing order, effectively representing the early stages of the learning curve (Soares et al., 2001; Fürnkranz & Petrak, 2001). This is conceptually related to the scaling laws observed in deep neural networks (Kaplan et al., 2020) and large language models (Zhang et al., 2024), which describe the predictable relationship between model performance and, among other factors, dataset size. Subsampling landmarks can thus be viewed as a localized and practical proxy for these scaling behaviors, enabling performance forecasting without requiring full-scale training. Similar ideas have been applied for hyperparameter optimization (Domhan et al., 2015; Jamieson & Talwalkar, 2016; Klein et al., 2017; Li et al., 2018), which use partial learning curves to stop training poor configurations early. Such methods, however, remain inherently single-objective and cannot directly address the multi-objective settings considered in this work.

Multi-Task and Meta-Reinforcement Learning Reinforcement learning is a powerful tool for sequential decision-making problems, but it often struggles with generalization to new (unknown)

108 tasks, requiring large amounts of data to readapt effectively. Two areas address these limitations: multi-task reinforcement learning (MTRL) (Teh et al., 2017; Sodhani et al., 2021) and meta-
 109 reinforcement learning (Meta-RL) (Finn et al., 2017; Nichol et al., 2018; Wang et al., 2024). MTRL
 110 trains a single policy across a distribution of tasks, leveraging shared structure to improve general-
 111 ization and learning efficiency. In contrast, Meta-RL focuses on learning a policy that can rapidly
 112 adapt to new tasks using limited data, typically by encoding task-specific information into its in-
 113 ternal state or parameters. In this work, we focus on MTRL, as our goal is to evaluate policies on
 114 previously unseen datasets without further adaptation at test time.

116 **Multi-Objective Reinforcement Learning** Multi-objective reinforcement learning (MORL) ex-
 117 tends standard RL by optimizing policies with respect to multiple, often conflicting objectives rather
 118 than a single reward. Prior research on MORL, often combined with meta-learning, has largely
 119 relied on scalarization or objective preferences, requiring weight sweeps across many preferences
 120 to approximate the Pareto front (Lu et al., 2024; Wang et al., 2024; Liu & Qian, 2021; Chen et al.,
 121 2019). Because each weight vector defines a different scalar objective, changing preferences gen-
 122 erally requires another sweep (i.e., additional fine-tuning runs), so computation grows with each
 123 revision. By contrast, we target Pareto coverage in a single, efficient run.

124 **Hyperparameter Optimization** Work in hyperparameter optimization (HPO), often overlapping
 125 with neural architecture search (NAS), frequently leverages early training signals to discard low-
 126 promising configurations and reduce computational cost (Falkner et al., 2018; Li et al., 2020; Awad
 127 et al., 2021; Wistuba et al., 2022). Standard HPO methods, however, are fundamentally single-
 128 objective, and extending them to multi-objective settings typically relies on scalarization. As shown
 129 by Schmucker et al. (2021), scalarization-based adaptations usually perform significantly worse than
 130 methods explicitly designed for multi-objective search, highlighting a key limitation of conventional
 131 HPO techniques in scenarios requiring Pareto-efficient model selection.

133 3 PROBLEM STATEMENT

135 Consider a target dataset \mathcal{D} and a set \mathcal{X} of candidate pretrained language models to be fine-tuned.
 136 Then, given n metrics of interest (objectives), the problem can be formulated as the following multi-
 137 objective optimization problem:

$$\begin{aligned} \min_{x \in \mathcal{X}} \quad & (f_1(x, \mathcal{D}), \dots, f_n(x, \mathcal{D})) \\ \text{s.t.} \quad & f_i(x, \mathcal{D}) \leq f_i^{\max} \text{ for all } i = 1, \dots, n, \end{aligned} \quad (1)$$

141 where $f_i(x, \mathcal{D})$ represents the value of the i -th objective function after fine-tuning the pretrained
 142 model $x \in \mathcal{X}$ on the task-specific dataset \mathcal{D} , and f_i^{\max} denotes an arbitrary upper bound for that
 143 objective.

145 Common objectives may include final test loss, training time (cost), inference throughput, number
 146 of model parameters, and resource usage (i.e., number of GPUs). It is very common that some
 147 objectives conflict with each other. For example, achieving a lower test loss may require longer
 148 training time or more GPUs. For this reason, there is typically no single solution that is optimal
 149 across all objectives. Hence, the notion of optimality is based on Pareto-dominance, or simply
 150 dominance, as defined below.

151 **Definition 1** (Weak dominance). A solution $x_1 \in \mathcal{X}$ weakly dominates another solution $x_2 \in \mathcal{X}$,
 152 denoted $x_1 \succeq x_2$, if $f_i(x_1, \mathcal{D}) \leq f_i(x_2, \mathcal{D})$ for all $i \in \{1, \dots, n\}$. That is, x_1 is not worse than x_2
 153 in all objectives.

154 **Definition 2** (Pareto-dominance). A solution $x_1 \in \mathcal{X}$ dominates another solution $x_2 \in \mathcal{X}$, denoted
 155 $x_1 \succ x_2$, if $f_i(x_1, \mathcal{D}) \leq f_i(x_2, \mathcal{D})$ for all $i \in \{1, \dots, n\}$, with at least one of these inequalities
 156 holding strictly. That is, there is $j \in \{1, \dots, n\}$ such that $f_j(x_1, \mathcal{D}) < f_j(x_2, \mathcal{D})$. In other words,
 157 x_1 dominates x_2 if x_1 is not worse than x_2 in all objectives, but it is better in at least one of them.

158 **Definition 3** (Pareto-optimal). A model $x^* \in \mathcal{X}$ is Pareto-optimal if there is no other $x \in \mathcal{X}$ that
 159 dominates x^* .

160 One way to evaluate and compare sets of candidate solutions is to use the *hypervolume indicator*
 161 (Guerreiro et al., 2021; Emmerich et al., 2005), which quantifies the volume of the objec-
 162 tive space weakly dominated by a set of solutions and bounded above by a given reference point

162 $r = [f_1^{\max}, \dots, f_n^{\max}]^\top$. For any subset $X \subset \mathcal{X}$, the hypervolume indicator is denoted as $H_{\mathcal{D}}(X, r)$.
 163 Intuitively, each solution in X defines a box in the objective space, with one corner at the objective
 164 values of the solution and the opposite corner at the reference point r . It is defined formally as
 165 follows:

166 **Definition 4** (Hypervolume indicator). *Given a set of points $S \subset \mathbb{R}^n$ and a reference point $r \in \mathbb{R}^n$,
 167 the hypervolume indicator of S is the measure of the region weakly dominated by S and bounded
 168 above by r , i.e.,*

$$169 \quad 170 \quad 171 \quad 172 \quad 173 \quad H(S, r) = \Lambda \left(\bigcup_{\substack{p \in S \\ p \leq r}} [p, r] \right),$$

174 where $\Lambda(\cdot)$ denotes the Lebesgue measure and $[p, r] = \{q \in \mathbb{R}^n \mid \forall i = 1, \dots, n : p_i \leq q_i \leq r_i\}$
 175 denotes the box delimited below by $p \in S$ and above by r .

176 It has been shown that maximizing the hypervolume indicator is equivalent to finding the Pareto
 177 optimal set (Guerreiro et al., 2021; Liu et al., 2019). Figure 1 illustrates this with a practical com-
 178 parison, showing that the Pareto-optimal set has the highest hypervolume. Thus, the problem in (1)
 179 can be reformulated as a single-objective problem as follows:

$$180 \quad 181 \quad \max_{X \subset \mathcal{X}} H_{\mathcal{D}}(X, r) \quad (2)$$

182 A trivial solution would involve fine-tuning all
 183 models on the target dataset (i.e., $X = \mathcal{X}$),
 184 but this is computationally intractable. To en-
 185 courage computational efficiency, we introduce
 186 a regularization term penalizing the number of
 187 selected pretrained models:

$$188 \quad 189 \quad \max_{X \subset \mathcal{X}} H_{\mathcal{D}}(X, r) - \lambda |X| \quad (3)$$

190 where $\lambda > 0$ is a user-defined penalty factor. To
 191 ensure that the optimal solution for the prob-
 192 lem in Equation 3 contains exactly all Pareto-
 193 optimal solutions, λ must satisfy the following
 194 theorem, proved in Appendix H:

195 **Theorem 1** (Condition on λ). *The optimal so-
 196 lution $X^* \subset \mathcal{X}$ of problem 3 contains only and
 197 exactly all Pareto-optimal solutions if and only
 198 if:*

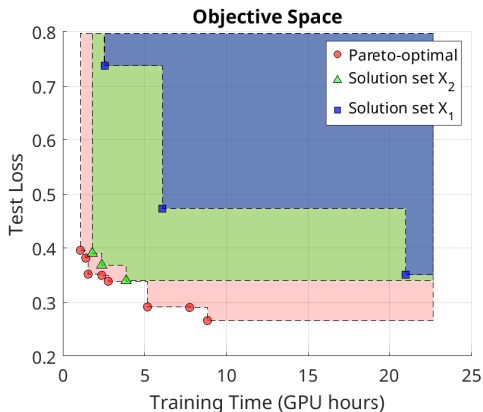
$$199 \quad 200 \quad 0 < \lambda \leq \min_{x \in X^*, X \subseteq X^*} \Delta H_{\mathcal{D}}(x \mid X), \quad (4)$$

201 where $\Delta H_{\mathcal{D}}(x \mid X)$ denotes the incremental
 202 hypervolume obtained by adding the Pareto-optimal solution x to the subset $X \subseteq X^*$.

203 In other words, the penalty λ must be smaller than or equal to the smallest incremental hypervolume
 204 gained by including a new Pareto-optimal solution into the subset of selected solution candidates.
 205 If this condition holds, the optimal solution set will include only all Pareto-optimal solutions. The
 206 next sections present empirical strategies for quickly providing near-Pareto optimal solutions.

209 4 LANDMARK FINE-TUNING

211 Fine-tuning a pretrained model on a task-specific dataset is inevitable if one desires to evaluate its
 212 true performance and determine its suitability for a given application. However, as discussed earlier,
 213 evaluating every candidate model is computationally expensive. Prior work on hyperparameter op-
 214 timization suggests that evaluating models for only a single epoch can already be a good proxy for
 215 its final performance (Egele et al., 2023). However, training for just one epoch may still consume
 significant resources, particularly for large models and datasets.



207 Figure 1: Illustration of the hypervolume indica-
 208 tor in a bi-objective setting, corresponding to the
 209 shaded areas. Set X_2 yields a larger hypervolume
 210 than X_1 , which is closer to the true Pareto front.

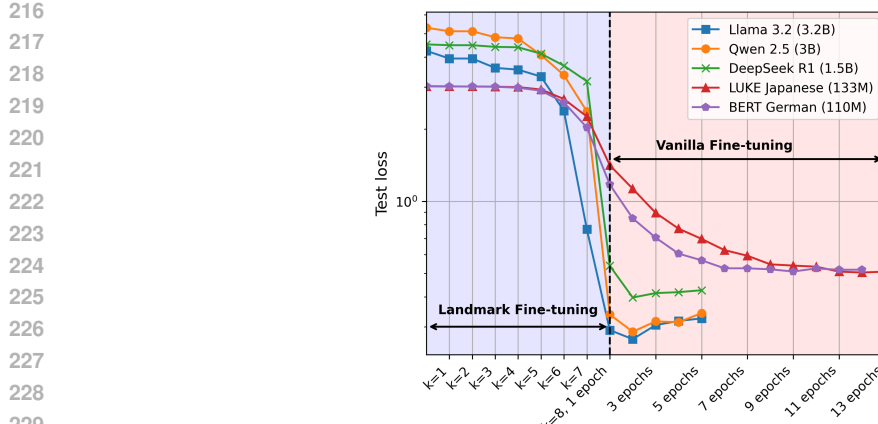


Figure 2: Landmark fine-tuning on the 20 Newsgroups dataset using $K = 8$. Larger models start off worse but eventually outperform smaller ones. Notably, models that improve quickly early on tend to achieve lower final loss, suggesting that the initial segments of the learning curves can help predict the overall performance.

To mitigate this inefficiency and allow for even earlier identification of unpromising candidates, we propose *landmark fine-tuning*, a lightweight fine-tuning strategy based on subsampling landmarks to obtain early estimates of objective values $f_i(x, \mathcal{D})$ for $i \in \{1 \dots n\}$.

Given that the target dataset \mathcal{D} has a training and a test split, namely $\mathcal{D}^{\text{train}}$ and $\mathcal{D}^{\text{test}}$, the core idea is to split $\mathcal{D}^{\text{train}}$ into K exponentially larger subsets $\mathcal{D}_1 \dots \mathcal{D}_K$. Each subset \mathcal{D}_k contains $\lfloor \frac{1}{2^{(K-k)}} |\mathcal{D}^{\text{train}}| \rfloor$ samples, where $\mathcal{D}_k \subset \mathcal{D}_{k+1}$ for $k = 1 \dots K-1$.

The process starts by fine-tuning a pretrained model on \mathcal{D}_1 for a *single epoch* and evaluating it on the entire $\mathcal{D}^{\text{test}}$. Next, it continues the fine-tuning process on the subsequent (larger) subset \mathcal{D}_2 , repeating this process up to \mathcal{D}_K (100% of the training dataset). After that, we continue fine-tuning the model for more epochs until convergence or other stop criterion.

Figure 2 shows a practical example of landmark fine-tuning with $K = 8$, depicting the learning curves (test cross-entropy loss) of five different pretrained models fine-tuned on the 20 Newsgroups dataset. Two non-English LLMs are included to illustrate the performance of less suitable models on an English dataset. Notice that larger models start with higher losses than smaller ones, but eventually overtake them, achieving lower final losses. In addition, among the larger models, those that improve more quickly in the initial steps tend to achieve better final test loss. These observations support the idea that early segments of the training curve can indeed be predictive of final loss, with predictions becoming more accurate as additional curve segments are provided.

5 META-LEARNED RESOURCE ALLOCATION VIA REINFORCEMENT LEARNING

Although landmark fine-tuning provides early performance estimates, it is still necessary to determine when to continue training a candidate model or not, based on partial information collected so far. To address this, we train a reinforcement learning agent on a meta-dataset of historical fine-tuning trajectories, covering a diverse set of pretrained LLMs and downstream tasks. The agent learns to allocate training resources by tracking how performance evolves across landmark steps, enabling fast and generalizable identification of near-Pareto-optimal models.

Observation space The observation space defines the information available to the RL agent at each decision step. At each time step t , the RL agent observes, for every candidate model, the objectives of interest (e.g., the elapsed training time and test loss), together with the number of fine-tuning steps that each candidate has completed.

270 **Action space** The action space specifies the set of decisions available to the RL agent at each
 271 step. For each time step t , the agent selects an action $a_t \in \{1, \dots, m\}$, representing the index of a
 272 candidate pretrained model, where m is the total number of candidates. Each action corresponds to
 273 allocating one additional fine-tuning step to the selected model. To improve exploration efficiency,
 274 we apply invalid action masking for terminated models (Huang & Ontañón, 2022). A binary mask
 275 specifies which models remain available for selection. The policy then samples only from this valid
 276 subset by setting the probability of invalid actions to zero. This prevents wasted trials on completed
 277 models and makes the exploration phase more efficient, as the agent can focus its decisions on
 278 candidates that may still yield improvements.

279 **Termination condition** An episode corresponds to the full search process and terminates when all
 280 Pareto-optimal models have been fully fine-tuned¹, thereby achieving the maximum hypervolume.
 281 **This termination condition is only necessary during policy training, where the agent has access**
 282 **to privileged information that indicates when the Pareto frontier has been fully explored.** Thanks
 283 to invalid action masking, the episode is guaranteed to terminate within a finite number of steps,
 284 preventing the agent from getting stuck in infinite allocations to unproductive models.

285 **Training algorithm** For training the policy, we adopted a standard multi-task reinforcement learning
 286 setup, in which a single policy is optimized jointly across all training tasks. **Distral (distill and**
 287 **transfer learning), a framework for multi-task RL where the knowledge gained in one task is distilled**
 288 **into a shared policy, then transferred to other tasks via regularization using a Kullback-Leibler (KL)**
 289 **divergence.** As the underlying optimizer, we adopted Proximal Policy Optimization (PPO) (Schul-
 290 man et al., 2017), which provides stable on-policy updates and performs reliably in multi-task set-
 291 tings. **combining its stability with cross-task transfer from Distral.**

292 **Rewards** The reward function links our multi-objective search problem to the policy’s learning
 293 process. Let $X_t \subseteq \mathcal{X}$ be the set of fully fine-tuned models by time step t , and let T be the length of
 294 the episode. Inspired by equation 3, we could initially define a sparse reward function

$$r_t = \begin{cases} H_{\mathcal{D}}(X_t) - \lambda|X_t| & \text{if } t = T \\ 0 & \text{otherwise} \end{cases}, \quad (5)$$

301 so that PPO would maximize

$$\max_{\theta} \mathbb{E}_{\rho \sim \pi_{\theta}} \left[\sum_{t=0}^T \gamma^t r_t \right] = \mathbb{E}_{\rho \sim \pi_{\theta}} \left[H_{\mathcal{D}}(X_T) - \lambda|X_T| \right], \quad (6)$$

306 where ρ is a trajectory sampled using policy π_{θ} , and γ is the discount factor.

307 Because an episode terminates only after all Pareto-optimal models have been fully fine-tuned,
 308 $H_{\mathcal{D}}(X_T)$ is identical for every trajectory and, therefore, constant. The objective thus collapses
 309 to minimizing the expected number of models evaluated, i.e., $\mathbb{E}[-|X_T|]$. Notice that λ also vanishes
 310 in this sparse reward setting, so we do not need to estimate it. Finally, to make the reward positive
 311 and incentivize faster convergence to the optimal, we adopted the following sparse reward function:

$$r_t = \begin{cases} \frac{|\mathcal{X} \setminus X_t|}{\Delta_t} & \text{if } t = T \\ 0 & \text{otherwise} \end{cases}, \quad (7)$$

316 where Δ_t is the cumulative wall-clock time spent up to time step t . In other words, we seek to
 317 maximize the number of pretrained models not fully fine-tuned, divided by the time spent to find
 318 all Pareto-optimal models. This produces a positive and well-scaled learning signal and preserves
 319 the optimal solution of equation 3, as the highest reward is obtained when $X_T = X^*$. Appendix D
 320 presents additional evidence showing that the proposed reward signal in equation 7 leads PPO to
 321 converge to the optimal solution during the training phase.

322 ¹A model is considered fully fine-tuned when its validation loss stops improving for a fixed number of
 323 consecutive epochs.

324 **Algorithm 1:** LAMPS Search Procedure

325 **Input** : Training dataset $\mathcal{D}^{\text{train}}$, validation dataset \mathcal{D}^{val}

326 **Input** : Policy π_θ

327 **Output:** Set of non-dominated fine-tuned models \hat{X}^*

328 1 Initialize time step $t \leftarrow 0$;

329 2 Initialize the set of selected models $X \leftarrow \emptyset$;

330 3 Evaluate candidate models on \mathcal{D}^{val} and construct the initial state s_0 ;

331 4 **while** search budget not exhausted **do**

332 5 Select action $a_t \leftarrow \arg \max_a \pi_\theta(a \mid s_t)$;

333 6 Fine-tune model x_{a_t} for one additional fine-tuning step on $\mathcal{D}_{k+1}^{\text{train}}$;

334 7 Evaluate updated performance on \mathcal{D}^{val} ;

335 8 **if** stopping criterion met for model x_{a_t} **then**

336 9 $X \leftarrow X \cup \{x_{a_t}\}$

337 10 Update environment state s_{t+1} ;

338 11 $t \leftarrow t + 1$;

339 12 $\hat{X}^* = \{x \in X \mid \nexists y \in X : y \succ x\}$;

340 13 **return** \hat{X}^* ;

341

342

343

344

345

346 **Meta-dataset** To meta-train a policy capable of efficiently identifying (or approximating) the
 347 Pareto-optimal set for new task-specific datasets, we conducted a fine-tuning campaign and
 348 constructed a meta-dataset containing fully recorded learning curves of 70 pretrained LLMs, each land-
 349 mark fine-tuned on multiple datasets (see Appendix E). This setup enables the agent to query arbi-
 350 trary trajectories during its training, allowing the use of on-policy algorithms such as PPO.

351 **Deployment (search procedure)** Given a trained policy π_θ and a target dataset \mathcal{D} , the search
 352 procedure of LAMPS is outlined in Algorithm 1. The process begins by constructing the initial
 353 state s_0 through zero-shot evaluation of all candidate models on the test split. It also serves as a
 354 sanity check to ensure that each model is available, downloaded properly, and compatible with the
 355 available hardware (and drivers) where the search will be performed. The policy then proceeds by
 356 selecting and executing new actions until the search budget is exhausted. In the end, dominated
 357 solutions are filtered out, so that only the best trade-offs are presented to the user.

360 6 EXPERIMENTS AND RESULTS

361 This section presents our experimental setup and main findings, demonstrating how well the trained
 362 policy generalizes to held-out datasets. The experiments presented in this section All experiments in
 363 this paper were conducted on eight NVIDIA A100 (40 GB) GPUs.

365 6.1 EXPERIMENTAL SETUP

367 **Pretrained LLMs** We tested 70 different pretrained language models, spanning models from a
 368 few million parameters (ALBERT) to eight billion parameters (DeepSeek-R1). These models cover
 369 languages such as English, Japanese, Chinese, German, Dutch, Spanish, and many of which are
 370 multilingual. The complete list of pretrained models can be found in Appendix F. We did not
 371 considered any Mixture-of-Experts (MoE) models, as they are usually more challenging to fine-tune
 372 and more prone to overfitting (Fedus et al., 2022; Shen et al., 2024).

373 **Fine-tuning Setup** We adopted full-model fine-tuning, which updates all parameters of the pre-
 374 trained models. Although parameter-efficient methods such as LoRA (Hu et al., 2022) or layer-
 375 freezing strategies can significantly reduce computational overhead, full fine-tuning often leads to
 376 better downstream performance (Zhang et al., 2024; Shuttleworth et al., 2024). All models were
 377 fine-tuned under identical hyperparameter settings. See Appendix C for details.

378 **Reinforcement Learning Setup** We used the following libraries: Stable-Baselines3 (SB3) for
 379 PPO implementation and invalid action masking (Raffin et al., 2021), and the Gymnasium library
 380 for standardized environment definition (Towers et al., 2024).
 381

382 **Objectives** For the optimization criteria, we focus primarily on two objectives: validation loss
 383 (measured via cross-entropy) and model size (in number of parameters) training-time required for
 384 completing the fine-tuning. Validation loss is a widely accepted proxy for task-specific performance,
 385 and model size training-time serves as a practical and measurable approximation for other metrics,
 386 such as VRAM model size, inference throughput, deployment cost, etc. These choices are not fixed
 387 for LAMPS, as the framework is objective-agnostic. Hence, any measurable objectives can be
 388 used², as long as the corresponding metrics are recorded in the meta-dataset. In Appendix B we
 389 show additional results for machine translation, considering two and three objectives.
 390

391 **Reference point** We set the reference point by taking the worst values of the chosen objectives
 392 across the meta-dataset and adding a 10% margin. This reference point is used only during policy
 393 training for computing the hypervolume. It is not required at test time when evaluating the trained
 394 policy (Algorithm 1).
 395

396 **Baselines** To our knowledge, no prior work has explored the same multi-objective optimization
 397 problem. Hence, a direct comparison with other existing methods was not possible. For this reason,
 398 We compared LAMPS with four three basic baselines:
 399

- **Blind**: chooses actions at random. Its performance serves as a lower bound on performance and represents the worst-case scenario.
- **Oracle**: assumes prior knowledge of the Pareto-optimal models for a given task. The performance of this approach represents the best-case scenario. In practice, this information is not available and serves only as a theoretical upper bound.
- **ZigZag**: a simple heuristic that sorts all candidate models by their number of parameters, then selects them in an alternating order (from largest to smallest and vice versa) in an attempt to quickly increase the covered hypervolume.
- **MO-ASHA**: multi-objective asynchronous successive halving, combined with ϵ -net exploration strategy (Schmucker et al., 2021).

411 **Evaluation Method** To evaluate LAMPS’s generalization, we employed leave-one-out cross-
 412 validation (Hastie et al., 2009), where one dataset is held exclusively for testing. For each fold,
 413 the policy is trained on the remaining datasets for a fixed number of steps and then evaluated on the
 414 held-out dataset. This allows us to assess how well the learned policy transfers to previously un-
 415 seen tasks. To ensure robustness, this procedure was repeated five times, and we report the average
 416 performance across these runs.
 417

418 6.2 RESULTS

420 To evaluate the generalization of LAMPS to unseen datasets, Figure 3 reports the time required to
 421 reach 99%^{98%} of the optimal hypervolume in each held-out dataset. Recall that, in our problem
 422 formulation, achieving optimal hypervolume corresponds to identifying all Pareto-optimal models.
 423 For reference, we also include the time needed for an exhaustive search to complete. Across the
 424 twelve held-out tasks, LAMPS achieves the best performance in nine datasets (75%), whereas MO-
 425 ASHA wins only three (25%). Although MO-ASHA is the strongest baseline overall, its behavior
 426 is markedly less stable: on several datasets, its search time approaches the BLIND baseline, which
 427 never occurs with LAMPS.
 428

429 To illustrate the practical implications, consider the Amazon dataset: running an exhaustive search
 430 on a single A100 40GB NVIDIA GPU (\$3.67 hourly) would cost \$5,141.67, whereas LAMPS

431 ²Choosing only highly correlated objectives collapses the Pareto frontier, effectively reducing a multi-
 432 objective problem to a single-objective one. Since adding objectives increases search complexity, it is important
 433 to select conflicting and informative objectives to make the multi-objective formulation meaningful.

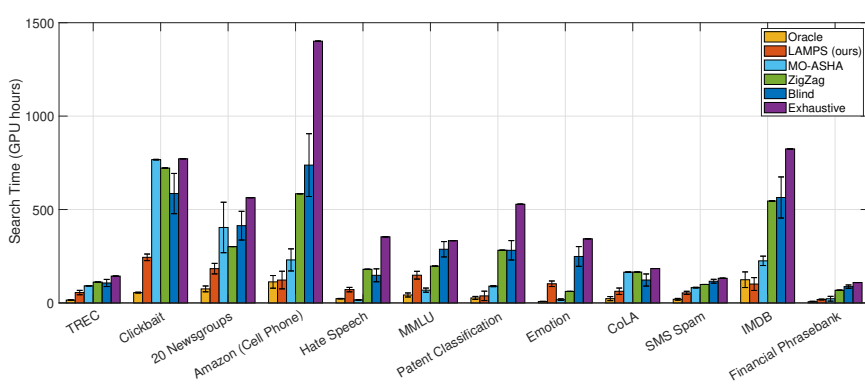


Figure 3: Mean time cost (in GPU hours) to reach **99%98%** of the optimal hypervolume indicator on held-out datasets. For reference, we also show the time to complete an exhaustive search. On average, LAMPS reduces the search time by **73.6%71%** compared to the exhaustive search, outperforming other feasible methods **in 9 out of 12 datasets** and being comparable to the **ORACLE** in **7 out of 9 datasets**.

reduces the cost to just \$449.58 with only a 1% degradation in the hypervolume. **The strongest competing baseline, MO-ASHA, would cost \$845.20 to reach the same performance.**

Figure 4 provides further insight by tracking the progression of the average hypervolume over search time. For comparability, hypervolume values are normalized by the maximum hypervolume, and we report the *hypervolume loss* (1 – normalized hypervolume) in logarithmic scale to highlight when the policy reaches optimality. Although LAMPS does not always reach optimality in a timely manner (compared to the other baselines), it clearly achieves near-optimal solutions quickly, eventually faster than ORACLE. This ability to deliver high-quality solutions at a fraction of the cost makes LAMPS the best trade-off between efficiency and solution quality, positioning it as a pragmatic and strong tool for practitioners.

Moreover, in multi-objective applications, the end user must ultimately select a preferred solution from the Pareto front, often revisiting trade-offs as requirements, constraints, or business priorities. By quickly providing a diverse set of strong candidates, LAMPS not only accelerates the search, but also enables practitioners to reconsider or change their choice later without having to undergo another expensive search, offering both flexibility and long-term practical value.

7 CONCLUSION

We presented LAMPS, a novel and open-source AutoML framework for efficiently selecting pre-trained language models for fine-tuning, framing it as a multi-objective optimization problem. By combining landmark fine-tuning and meta-learning via reinforcement learning, LAMPS significantly reduces search costs while maintaining near-optimal performance. Experiments show that LAMPS reduces search time by **73%71%** on average with minimal hypervolume degradation. To our knowledge, this is the first framework to deliver Pareto-efficient selection and fine-tuning for LLMs, establishing a new baseline for cost-aware AutoML and paving the way toward sustainable, high-performance deployment of foundation models.

REFERENCES

Mathias M. Adankon and Mohamed Cheriet. Model selection for the ls-svm. application to handwriting recognition. *Pattern Recognition*, 42(12):3264–3270, 2009. ISSN 0031-3203. doi: <https://doi.org/10.1016/j.patcog.2008.10.023>. URL <https://www.sciencedirect.com/science/article/pii/S0031320308004494>. New Frontiers in Handwriting Recognition.

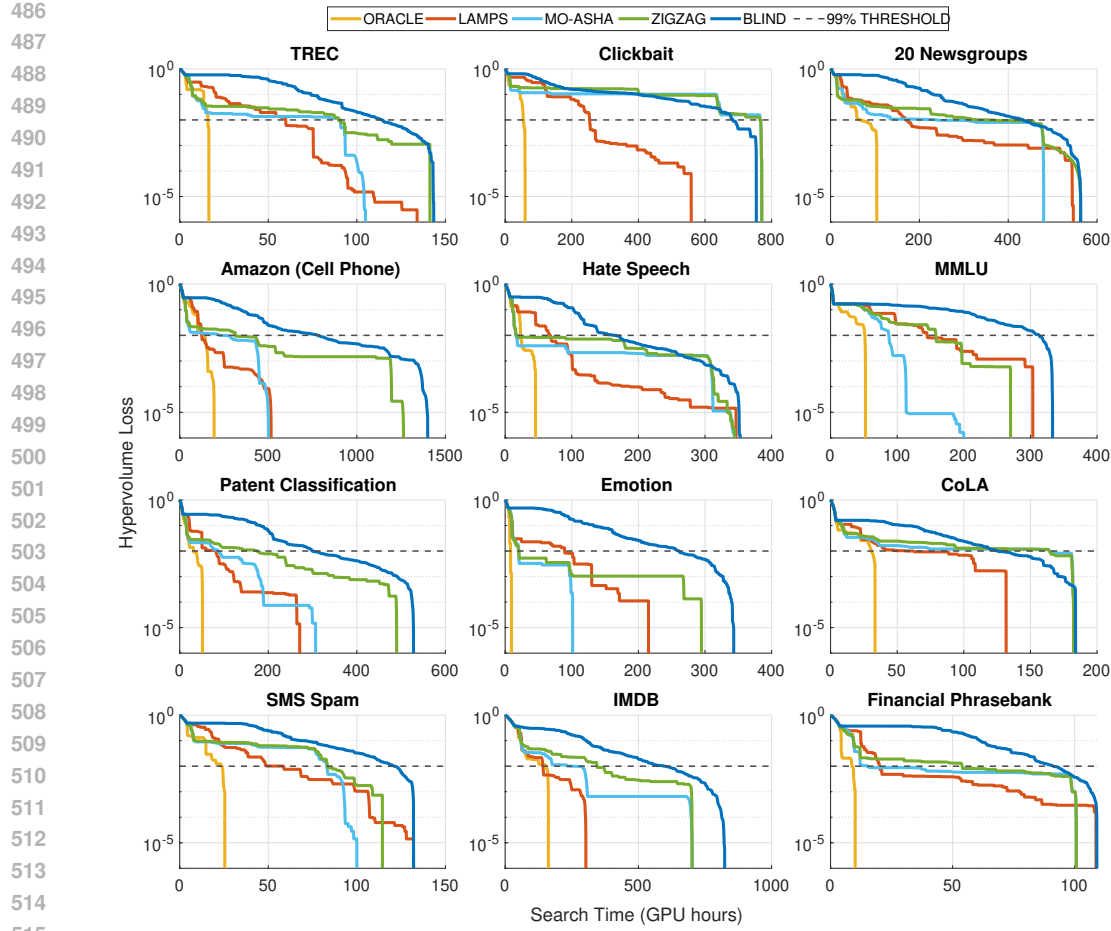


Figure 4: Evolution of the mean hypervolume indicator on held-out datasets as a function of search budget. LAMPS rapidly identifies near-optimal solutions (dashed line) in [nineseven](#) out of [twelve nine](#) cases, demonstrating strong generalization capabilities, even when trained on a small meta-dataset.

Armen Aghajanyan, Akshat Shrivastava, Anchit Gupta, Naman Goyal, Luke Zettlemoyer, and Sonal Gupta. Better fine-tuning by reducing representational collapse. *arXiv preprint arXiv:2008.03156*, 2020.

Noor Awad, Neeratyoy Mallik, and Frank Hutter. Dehb: Evolutionary hyperband for scalable, robust and efficient hyperparameter optimization. In Zhi-Hua Zhou (ed.), *Proceedings of the Thirtieth International Joint Conference on Artificial Intelligence, IJCAI-21*, pp. 2147–2153. International Joint Conferences on Artificial Intelligence Organization, 8 2021. doi: 10.24963/ijcai.2021/296. URL <https://doi.org/10.24963/ijcai.2021/296>. Main Track.

Alain Biem. A model selection criterion for classification: application to hmm topology optimization. In *Proceedings of the Seventh International Conference on Document Analysis and Recognition - Volume 1*, ICDAR '03, pp. 104, USA, 2003. IEEE Computer Society. ISBN 0769519601.

Hamparsum Bozdogan. Model selection and akaike's information criterion (aic): The general theory and its analytical extensions. *Psychometrika*, 52(3):345–370, 1987. doi: 10.1007/BF02294361. URL <https://doi.org/10.1007/BF02294361>.

Pavel Brazdil and Christophe Giraud-Carrier. Metalearning and algorithm selection: progress, state of the art and introduction to the 2018 special issue. *Machine learning*, 107:1–14, 2018.

540 Pavel Brazdil, Jan N. van Rijn, Carlos Soares, and Joaquin Vanschoren. *Dataset Characteristics (Metafeatures)*, pp. 53–75. Springer International Publishing, Cham, 2022. ISBN 978-3-030-67024-5. doi: 10.1007/978-3-030-67024-5_4. URL https://doi.org/10.1007/978-3-030-67024-5_4.

544 Pavel B. Brazdil, Carlos Soares, and Joaquim Pinto Da Costa. Ranking learning algorithms: using
545 ibl and meta-learning on accuracy and time results. *Mach. Learn.*, 50(3):251–277, March 2003.
546 ISSN 0885-6125. doi: 10.1023/A:1021713901879. URL <https://doi.org/10.1023/A:1021713901879>.

549 Abhijnan Chakraborty, Bhargavi Paranjape, Sourya Kakarla, and Niloy Ganguly. Stop clickbait: De-
550 tecting and preventing clickbaits in online news media. In *Advances in Social Networks Analysis*
551 and Mining (ASONAM), 2016 IEEE/ACM International Conference on, pp. 9–16. IEEE, 2016.

552 Olivier Chapelle, Vladimir Vapnik, and Yoshua Bengio. Model selection for small sample regres-
553 sion. *Machine Learning*, 48(1):9–23, 2002. doi: 10.1023/A:1013943418833. URL <https://doi.org/10.1023/A:1013943418833>.

556 Xi Chen, Ali Ghadirzadeh, Mårten Björkman, and Patric Jensfelt. Meta-learning for multi-objective
557 reinforcement learning. In *2019 IEEE/RSJ International Conference on Intelligent Robots and*
558 *Systems (IROS)*, pp. 977–983. IEEE Press, 2019. doi: 10.1109/IROS40897.2019.8968092. URL
559 <https://doi.org/10.1109/IROS40897.2019.8968092>.

560 Aakanksha Chowdhery, Sharan Narang, Jacob Devlin, Maarten Bosma, Gaurav Mishra, Adam
561 Roberts, Paul Barham, Hyung Won Chung, Charles Sutton, Sebastian Gehrmann, et al. Palm:
562 Scaling language modeling with pathways. *Journal of Machine Learning Research*, 24(240):
563 1–113, 2023.

564 Thomas Davidson, Dana Warmsley, Michael Macy, and Ingmar Weber. Automated hate speech
565 detection and the problem of offensive language. In *Proceedings of the 11th International AAAI*
566 *Conference on Web and Social Media*, ICWSM ’17, pp. 512–515, 2017.

568 Lucas B. V. de Amorim, George D. C. Cavalcanti, and Rafael M. O. Cruz. Meta-scaler: A meta-
569 learning framework for the selection of scaling techniques. *IEEE Transactions on Neural Net-*
570 *works and Learning Systems*, 36(3):4805–4819, 2025. doi: 10.1109/TNNLS.2024.3366615.

572 DeepSeek-AI et al. Deepseek-r1: Incentivizing reasoning capability in llms via reinforcement learn-
573 ing, 2025. URL <https://arxiv.org/abs/2501.12948>.

574 Gianna M. Del Corso, Antonio Gullí, and Francesco Romani. Ranking a stream of news. In *Pro-
575 ceedings of the 14th International Conference on World Wide Web*, WWW ’05, pp. 97–106,
576 New York, NY, USA, 2005. Association for Computing Machinery. ISBN 1595930469. doi:
577 10.1145/1060745.1060764. URL <https://doi.org/10.1145/1060745.1060764>.

579 Tobias Domhan, Jost Tobias Springenberg, and Frank Hutter. Speeding up automatic hyperparam-
580 eter optimization of deep neural networks by extrapolation of learning curves. In *Proceedings*
581 *of the 24th International Conference on Artificial Intelligence*, IJCAI’15, pp. 3460–3468. AAAI
582 Press, 2015. ISBN 9781577357384.

583 Romain Egele, Isabelle Guyon, Yixuan Sun, and Prasanna Balaprakash. Is one epoch all you need
584 for multi-fidelity hyperparameter optimization? *arXiv preprint arXiv:2307.15422*, 2023.

586 Michael Emmerich, Nicola Beume, and Boris Naujoks. An emo algorithm using the hyper-
587 volume measure as selection criterion. In *Proceedings of the Third International Conference*
588 *on Evolutionary Multi-Criterion Optimization*, EMO’05, pp. 62–76, Berlin, Heidelberg, 2005.
589 Springer-Verlag. ISBN 3540249834. doi: 10.1007/978-3-540-31880-4_5. URL https://doi.org/10.1007/978-3-540-31880-4_5.

592 Stefan Falkner, Aaron Klein, and Frank Hutter. Bohb: Robust and efficient hyperparameter op-
593 timization at scale. In *International conference on machine learning*, pp. 1437–1446. PMLR,
2018.

594 Armin Farhadi, Roya Hatami, Mohammad Robat Mili, Christos Masouros, and Mehdi Bennis. A
 595 meta-learning approach for energy-efficient resource allocation and antenna selection in star-bd-
 596 ris aided wireless networks. *IEEE Wireless Communications Letters*, pp. 1–1, 2025. doi: 10.
 597 1109/LWC.2025.3543780.

598 William Fedus, Barret Zoph, and Noam Shazeer. Switch transformers: scaling to trillion parameter
 599 models with simple and efficient sparsity. *J. Mach. Learn. Res.*, 23(1), January 2022. ISSN
 600 1532-4435.

602 Chelsea Finn, Pieter Abbeel, and Sergey Levine. Model-agnostic meta-learning for fast adaptation
 603 of deep networks. In *Proceedings of the 34th International Conference on Machine Learning -*
 604 *Volume 70*, ICML'17, pp. 1126–1135. JMLR.org, 2017.

605 Johannes Fürnkranz and Johann Petrak. An evaluation of landmarking variants. In *Working Notes of*
 606 *the ECML/PKDD 2000 Workshop on Integrating Aspects of Data Mining, Decision Support and*
 607 *Meta-Learning*, pp. 57–68. Citeseer, 2001.

609 Johannes Fürnkranz, Josef Petrak, Pavel Brazdil, and Carlos Soares. On the use of fast subsam-
 610 pling estimates for algorithm recommendation. Technical report, Austrian Research Institute for
 611 Artificial Intelligence, 2002.

612 Alec Go, Richa Bhayani, and Lei Huang. Twitter sentiment classification using distant supervision.
 613 *CS224N project report, Stanford*, 1(12):2009, 2009.

615 Andreia P. Guerreiro, Carlos M. Fonseca, and Luís Paquete. The hypervolume indicator: Compu-
 616 tational problems and algorithms. *ACM Comput. Surv.*, 54(6), July 2021. ISSN 0360-0300. doi:
 617 10.1145/3453474. URL <https://doi.org/10.1145/3453474>.

618 Anna Gutowska. What are AI agents?, July 2024. URL <https://www.ibm.com/think/topics/ai-agents>. Accessed: 2025-02-07.

621 Trevor Hastie, Robert Tibshirani, and Jerome Friedman. *The elements of statistical learning: data*
 622 *mining, inference, and prediction*. Springer, New York, 2 edition, 2009. ISBN 978-0-387-84857-
 623 0. URL <https://hastie.su.domains/ElemStatLearn/>.

624 Jason Hepburn. Universal language model fine-tuning for patent classification. In Sunghwan Mac
 625 Kim and Xiuzhen (Jenny) Zhang (eds.), *Proceedings of the Australasian Language Technology*
 626 *Association Workshop 2018*, pp. 93–96, Dunedin, New Zealand, December 2018. URL <https://aclanthology.org/U18-1013/>.

629 Jordan Hoffmann, Sebastian Borgeaud, Arthur Mensch, Elena Buchatskaya, Trevor Cai, Eliza
 630 Rutherford, Diego de las Casas, Lisa Anne Hendricks, Johannes Welbl, Aidan Clark, Tom Hen-
 631 nigan, Eric Noland, Katherine Millican, George van den Driessche, Bogdan Damoc, Aurelia
 632 Guy, Simon Osindero, Karen Simonyan, Erich Elsen, Oriol Vinyals, Jack William Rae, and
 633 Laurent Sifre. An empirical analysis of compute-optimal large language model training. In
 634 Alice H. Oh, Alekh Agarwal, Danielle Belgrave, and Kyunghyun Cho (eds.), *Advances in Neu-*
 635 *ral Information Processing Systems*, 2022. URL <https://openreview.net/forum?id=iBBcRUL0APR>.

637 Edward J Hu, yelong shen, Phillip Wallis, Zeyuan Allen-Zhu, Yuanzhi Li, Shean Wang, Lu Wang,
 638 and Weizhu Chen. LoRA: Low-rank adaptation of large language models. In *International Con-*
 639 *ference on Learning Representations*, 2022. URL <https://openreview.net/forum?id=nZeVKeFYf9>.

641 Shengyi Huang and Santiago Ontañón. A closer look at invalid action masking in policy gradient
 642 algorithms. *The International FLAIRS Conference Proceedings*, 35, May 2022. ISSN 2334-
 643 0762. doi: 10.32473/flairs.v35i.130584. URL <http://dx.doi.org/10.32473/flairs.v35i.130584>.

646 Nishant Jain, Arun S. Suggala, and Pradeep Shenoy. Improving generalization via meta-learning
 647 on hard samples. In *2024 IEEE/CVF Conference on Computer Vision and Pattern Recognition*
 (CVPR), pp. 27590–27599, 2024. doi: 10.1109/CVPR52733.2024.02606.

648 Kevin Jamieson and Ameet Talwalkar. Non-stochastic best arm identification and hyperparameter
 649 optimization. In Arthur Gretton and Christian C. Robert (eds.), *Proceedings of the 19th*
 650 *International Conference on Artificial Intelligence and Statistics*, volume 51 of *Proceedings*
 651 *of Machine Learning Research*, pp. 240–248, Cadiz, Spain, 09–11 May 2016. PMLR. URL
 652 <https://proceedings.mlr.press/v51/jamieson16.html>.

653

654 A. Kalousis and M. Hilario. Model selection via meta-learning: a comparative study. In *Proceedings*
 655 *12th IEEE International Conference on Tools with Artificial Intelligence. ICTAI 2000*, pp. 406–
 656 413, 2000. doi: 10.1109/TAI.2000.889901.

657

658 Jared Kaplan, Sam McCandlish, Tom Henighan, Tom B. Brown, Benjamin Chess, Rewon Child,
 659 Scott Gray, Alec Radford, Jeffrey Wu, and Dario Amodei. Scaling laws for neural language
 660 models. *OpenAI blog*, 2020. URL <https://arxiv.org/abs/2001.08361>.

661

662 Aaron Klein, Stefan Falkner, Simon Bartels, Philipp Hennig, and Frank Hutter. Fast Bayesian Opti-
 663 mization of Machine Learning Hyperparameters on Large Datasets. In Aarti Singh and Jerry Zhu
 664 (eds.), *Proceedings of the 20th International Conference on Artificial Intelligence and Statistics*,
 665 volume 54 of *Proceedings of Machine Learning Research*, pp. 528–536. PMLR, 20–22 Apr 2017.
 666 URL <https://proceedings.mlr.press/v54/klein17a.html>.

667 Ken Lang. 20 newsgroups dataset, 1995. URL <http://qwone.com/~jason/20Newsgroups/>. Accessed: 2025-02-26.

668

669 Liam Li, Kevin Jamieson, Afshin Rostamizadeh, Ekaterina Gonina, Jonathan Ben-tzur,
 670 Moritz Hardt, Benjamin Recht, and Ameet Talwalkar. A system for massively parallel
 671 hyperparameter tuning. In I. Dhillon, D. Papailiopoulos, and V. Sze (eds.), *Pro-
 672 ceedings of Machine Learning and Systems*, volume 2, pp. 230–246, 2020. URL
 673 https://proceedings.mlsys.org/paper_files/paper/2020/file/a06f20b349c6cf09a6b171c71b88bbfc-Paper.pdf.

674

675 Lisha Li, Kevin Jamieson, Giulia DeSalvo, Afshin Rostamizadeh, and Ameet Talwalkar. Hyperband:
 676 A novel bandit-based approach to hyperparameter optimization. *Journal of Machine Learning
 677 Research*, 18(185):1–52, 2018. URL <http://jmlr.org/papers/v18/16-558.html>.

678

679 Fei-Yu Liu and Chao Qian. Prediction guided meta-learning for multi-objective reinforcement
 680 learning. In *2021 IEEE Congress on Evolutionary Computation (CEC)*, pp. 2171–2178. IEEE
 681 Press, 2021. doi: 10.1109/CEC45853.2021.9504972. URL <https://doi.org/10.1109/CEC45853.2021.9504972>.

682

683 Yang Liu, Jingxuan Wei, Xin Li, and Minghan Li. Generational distance indicator-based evolution-
 684 ary algorithm with an improved niching method for many-objective optimization problems. *IEEE
 685 Access*, 7:63881–63891, 2019. doi: 10.1109/ACCESS.2019.2916634.

686

687 Junlin Lu, Patrick Mannion, and Karl Mason. A meta-learning approach for multi-objective re-
 688 enforcement learning in sustainable home environments. In *European Conference on Artificial
 689 Intelligence (ECAI) 2024*, January 2024.

690

691 Wei Ma, Daoyuan Wu, Yuqiang Sun, Tianwen Wang, Shangqing Liu, Jian Zhang, Yue Xue, and
 692 Yang Liu. Combining fine-tuning and llm-based agents for intuitive smart contract auditing with
 693 justifications. *arXiv preprint arXiv:2403.16073*, 2024.

694

695 Andrew L. Maas, Raymond E. Daly, Peter T. Pham, Dan Huang, Andrew Y. Ng, and Christopher
 696 Potts. Learning word vectors for sentiment analysis. In Dekang Lin, Yuji Matsumoto, and
 697 Rada Mihalcea (eds.), *Proceedings of the 49th Annual Meeting of the Association for Compu-
 698 tational Linguistics: Human Language Technologies*, pp. 142–150, Portland, Oregon, USA, June
 699 2011. Association for Computational Linguistics. URL <https://aclanthology.org/P11-1015/>.

700

701 P. Malo, A. Sinha, P. Korhonen, J. Wallenius, and P. Takala. Good debt or bad debt: Detecting
 702 semantic orientations in economic texts. *Journal of the Association for Information Science and
 703 Technology*, 65, 2014.

702 Oded Maron and Andrew W. Moore. Hoeffding races: accelerating model selection search for
 703 classification and function approximation. In *Proceedings of the 7th International Conference on*
 704 *Neural Information Processing Systems*, NIPS'93, pp. 59–66, San Francisco, CA, USA, 1993.
 705 Morgan Kaufmann Publishers Inc.

706 Allan D R McQuarrie and Chih-Ling Tsai. *Regression and time series model selection*. WORLD
 707 SCIENTIFIC, 1998. doi: 10.1142/3573. URL <https://www.worldscientific.com/doi/abs/10.1142/3573>.

710 Marcio Monteiro, Charu Karakkaparambil James, Marius Kloft, and Sophie Fellenz. Characterizing
 711 text datasets with psycholinguistic features. In Yaser Al-Onaizan, Mohit Bansal, and Yun-
 712 Nung Chen (eds.), *Findings of the Association for Computational Linguistics: EMNLP 2024*, pp.
 713 14977–14990, Miami, Florida, USA, November 2024. Association for Computational Linguis-
 714 tics.

715 Alex Nichol, Joshua Achiam, and John Schulman. On first-order meta-
 716 learning algorithms, 2018. URL <https://openai.com/index/on-first-order-meta-learning-algorithms/>.

719 Long Ouyang, Jeffrey Wu, Xu Jiang, Diogo Almeida, Carroll Wainwright, Pamela Mishkin, Chong
 720 Zhang, Sandhini Agarwal, Katarina Slama, Alex Ray, John Schulman, Jacob Hilton, Fraser Kel-
 721 ton, Luke Miller, Maddie Simens, Amanda Askell, Peter Welinder, Paul F Christiano, Jan Leike,
 722 and Ryan Lowe. Training language models to follow instructions with human feedback. In S. Koyejo, S. Mohamed, A. Agarwal, D. Belgrave, K. Cho, and A. Oh (eds.), *Advances in*
 723 *Neural Information Processing Systems*, volume 35, pp. 27730–27744. Curran Associates, Inc.,
 724 2022. URL https://proceedings.neurips.cc/paper_files/paper/2022/file/b1efde53be364a73914f58805a001731-Paper-Conference.pdf.

727 Bernhard Pfahringer, Hilan Bensusan, and Christophe G. Giraud-Carrier. Meta-learning by land-
 728 marking various learning algorithms. In *Proceedings of the Seventeenth International Conference*
 729 *on Machine Learning*, ICML '00, pp. 743–750, San Francisco, CA, USA, 2000. Morgan Kauf-
 730 mann Publishers Inc. ISBN 1558607072.

731 Alec Radford, Jeffrey Wu, Rewon Child, David Luan, Dario Amodei, Ilya Sutskever, et al. Language
 732 models are unsupervised multitask learners. *OpenAI blog*, 1(8):9, 2019.

734 Colin Raffel, Noam Shazeer, Adam Roberts, Katherine Lee, Sharan Narang, Michael Matena, Yanqi
 735 Zhou, Wei Li, and Peter J. Liu. Exploring the limits of transfer learning with a unified text-to-text
 736 transformer. *J. Mach. Learn. Res.*, 21(1), January 2020. ISSN 1532-4435.

737 Antonin Raffin, Ashley Hill, Adam Gleave, Anssi Kanervisto, Maximilian Ernestus, and Noah
 738 Dormann. Stable-baselines3: Reliable reinforcement learning implementations. *Journal of*
 739 *Machine Learning Research*, 22(268):1–8, 2021. URL <http://jmlr.org/papers/v22/20-1364.html>.

741 Victor Sanh, Lysandre Debut, Julien Chaumond, and Thomas Wolf. Distilbert, a distilled version
 742 of bert: smaller, faster, cheaper and lighter, 2020. URL <https://arxiv.org/abs/1910.01108>.

745 Robin Schmucker, Michele Donini, Muhammad Bilal Zafar, David Salinas, and Cédric Archam-
 746 beau. Multi-objective asynchronous successive halving, 2021. URL <https://arxiv.org/abs/2106.12639>.

748 John Schulman, Filip Wolski, Prafulla Dhariwal, Alec Radford, and Oleg Klimov. Proximal policy
 749 optimization algorithms, 2017. URL <https://arxiv.org/abs/1707.06347>.

751 Sheng Shen, Le Hou, Yanqi Zhou, Nan Du, Shayne Longpre, Jason Wei, Hyung Won Chung,
 752 Barret Zoph, William Fedus, Xinyun Chen, Tu Vu, Yuexin Wu, Wuyang Chen, Albert Web-
 753 son, Yunxuan Li, Vincent Y Zhao, Hongkun Yu, Kurt Keutzer, Trevor Darrell, and Denny
 754 Zhou. Mixture-of-experts meets instruction tuning: A winning combination for large language
 755 models. In *The Twelfth International Conference on Learning Representations*, 2024. URL
<https://openreview.net/forum?id=6mLjDwYte5>.

756 Reece Shuttleworth, Jacob Andreas, Antonio Torralba, and Pratyusha Sharma. Lora vs full fine-
 757 tuning: An illusion of equivalence. *arXiv preprint arXiv:2410.21228*, 2024.

758

759 Carlos Soares, Johann Petrank, and Pavel Brazdil. Sampling-based relative landmarks: systematically
 760 test-driving algorithms before choosing. In Pavel Brazdil and Alíprio Jorge (eds.), *Progress in
 761 Artificial Intelligence*, pp. 88–95, Berlin, Heidelberg, 2001. Springer Berlin Heidelberg. ISBN
 762 978-3-540-45329-1.

763 Shagun Sodhani, Amy Zhang, and Joelle Pineau. Multi-task reinforcement learning with context-
 764 based representations. In Marina Meila and Tong Zhang (eds.), *Proceedings of the 38th Inter-
 765 national Conference on Machine Learning*, volume 139 of *Proceedings of Machine Learning
 766 Research*, pp. 9767–9779. PMLR, 18–24 Jul 2021. URL <https://proceedings.mlr.press/v139/sodhani21a.html>.

767

768 Yee Whye Teh, Victor Bapst, Wojciech Marian Czarnecki, John Quan, James Kirkpatrick, Raia
 769 Hadsell, Nicolas Heess, and Razvan Pascanu. Distral: robust multitask reinforcement learn-
 770 ing. In *Proceedings of the 31st International Conference on Neural Information Processing
 771 Systems*, NIPS’17, pp. 4499–4509, Red Hook, NY, USA, 2017. Curran Associates Inc. ISBN
 772 9781510860964.

773

774 Jörg Tiedemann. Parallel data, tools and interfaces in OPUS. In Nicoletta Calzolari, Khalid Choukri,
 775 Thierry Declerck, Mehmet Uğur Doğan, Bente Maegaard, Joseph Mariani, Asuncion Moreno,
 776 Jan Odijk, and Stelios Piperidis (eds.), *Proceedings of the Eighth International Conference on
 777 Language Resources and Evaluation (LREC’12)*, pp. 2214–2218, Istanbul, Turkey, May 2012.
 778 European Language Resources Association (ELRA). URL http://www.lrec-conf.org/proceedings/lrec2012/pdf/463_Paper.pdf.

779

780 Mark Towers, Ariel Kwiatkowski, Jordan Terry, John U Balis, Gianluca De Cola, Tristan Deleu,
 781 Manuel Goulão, Andreas Kallinteris, Markus Krimmel, Arjun KG, et al. Gymnasium: A standard
 782 interface for reinforcement learning environments. *arXiv preprint arXiv:2407.17032*, 2024.

783

784 Yasmen Wahba, Nazim Madhavji, and John Steinbacher. A comparison of svm against pre-trained
 785 language models (plms) for text classification tasks. In Giuseppe Nicosia, Varun Ojha, Emanuele
 786 La Malfa, Gabriele La Malfa, Panos Pardalos, Giuseppe Di Fatta, Giovanni Giuffrida, and Renato
 787 Umeton (eds.), *Machine Learning, Optimization, and Data Science*, pp. 304–313, Cham, 2023.
 788 Springer Nature Switzerland. ISBN 978-3-031-25891-6.

789

790 Qi Wang, Chengwei Zhang, and Bin Hu. Dynamic programming with meta-reinforcement learn-
 791 ing: a novel approach for multi-objective optimization. *Complex & Intelligent Systems*, 10(4):
 792 5743–5758, 2024. doi: 10.1007/s40747-024-01469-1. URL <https://doi.org/10.1007/s40747-024-01469-1>.

793

794 Shangshang Wang, Julian Asilis, Ömer Faruk Akgül, Enes Burak Bilgin, Ollie Liu, and Willie
 795 Neiswanger. Tina: Tiny reasoning models via lora, 2025. URL <https://arxiv.org/abs/2504.15777>.

796

797 Martin Wistuba, Arlind Kadra, and Josif Grabocka. Supervising the multi-fidelity race of hyperpa-
 798 rameter configurations. *Advances in Neural Information Processing Systems*, 35:13470–13484,
 799 2022.

800

801 Zhilin Yang. Xlnet: Generalized autoregressive pretraining for language understanding. *arXiv
 preprint arXiv:1906.08237*, 2019.

802

803 Biao Zhang, Zhongtao Liu, Colin Cherry, and Orhan Firat. When scaling meets LLM finetun-
 804 ing: The effect of data, model and finetuning method. In *The Twelfth International Confer-
 805 ence on Learning Representations*, 2024. URL <https://openreview.net/forum?id=5HCnKDeTws>.

806

807 Peng Zhao and Bin Yu. On model selection consistency of lasso. *Journal of Machine Learning Re-
 808 search*, 7(90):2541–2563, 2006. URL <http://jmlr.org/papers/v7/zhao06a.html>.

809

810 A LAMPS: GETTING STARTED
811812 This section demonstrates how to use LAMPS for a new, unseen dataset. The provided policy
813 was meta-trained across the datasets described in the main paper for a total of **10M45M** steps,
814 minimizing the following objectives: validation loss and **model size****training time**. Before running
815 it, make sure to have sufficient disk space (at least 2TB) for intermediate storage of models and
816 checkpoints. In addition, some models hosted on Hugging Face may require license agreements or
817 explicit acceptance terms. Ensure that the necessary access is granted to your user account prior to
818 execution.
819820 Listing 1: Running LAMPS for a new dataset.
821

```

822 # Create the Python environment
823 conda create -n lamps python=3.10
824 conda activate lamps

825 # Install dependencies
826 pip install -r requirements.txt

828 # Initiate the search using the trained policy
829 python eval.py --policy "policies/ALL-MTRL-30M_steps.zip" \
830   --dataset "stanfordnlp/imdb" \
831   --input-col "text" \
832   --target-col "label"
833
834
835
```

836 B ADDITIONAL EXPERIMENTS: MACHINE TRANSLATION
837838 To further assess the generality, objective-agnosticism, and scalability of LAMPS, we conducted
839 additional experiments in the domain of machine translation. Using 4x NVIDIA A100 (40GB)
840 GPUs, we constructed a meta-dataset comprising 38 translation directions from the OPUS Books
841 corpus, a collection of copyright-free literary texts spanning a wide range of languages (Tiedemann,
842 2012).844 B.1 TWO OBJECTIVES
845846 Table 1 reports the time (in GPU hours) to recover 99.9% of the optimal hypervolume when op-
847 timizing for model size and evaluation loss. The results show that LAMPS transfers meta-learned
848 knowledge effectively to the majority of held-out task-specific datasets, being comparable to the
849 ORACLE in 32 out of 38 cases.
850851 B.2 THREE OBJECTIVES
852853 To evaluate how well LAMPS scales to higher-dimensional objective spaces, we extend our analysis
854 to a three-objective setting involving model size, evaluation loss, and BLEU score. As shown in
855 Table 2, the ORACLE requires substantially more time to recover 99.9% of the optimal hypervolume
856 than in the 2D case. This increase reflects the expansion of the Pareto frontier (now a surface) when
857 BLEU is added, making the search space more challenging to find or approximate.
858859 Despite this increased complexity, LAMPS remains the strongest overall method by a large margin,
860 achieving the best search performance on 27 of 38 datasets (71%). Although MO-ASHA becomes
861 more competitive in this 3D setting, increasing its win rate to 10/38 (26%), its performance also
862 becomes significantly less stable: on several language pairs, it drops to the level of the BLIND base-
863 line, which has not been observed in the any of the 2D experiments. This widening performance gap
864 indicates that LAMPS scales more reliably and consistently as the dimensionality of the objective
865 space increases.

864
865 Table 1: Time in GPU-hours to recover 99.9% of the optimal hypervolume on held-out datasets,
866 optimizing for two objectives: model size and evaluation loss.

867 Dataset	868 Oracle	869 LAMPS (ours)	870 MO-ASHA	871 ZigZag	872 Blind	873 Exhaustive
874 DE-EN	875 46.0 ± 6.0	876 91.1 ± 5.9	877 50.7 ± 5.9	878 88.2	879 121.2 ± 3.2	880 123.9
881 DE-ES	882 18.2 ± 0.0	883 18.2 ± 0.0	884 35.5 ± 5.6	885 53.1	886 71.3 ± 2.4	887 73.6
889 DE-FR	890 18.4 ± 0.1	891 18.3 ± 0.1	892 36.4 ± 2.3	893 66.1	894 90.4 ± 3.0	895 93.0
901 DE-IT	902 20.7 ± 0.0	903 20.7 ± 0.0	904 38.0 ± 1.8	905 57.7	906 76.0 ± 1.7	907 77.1
914 DE-NL	915 12.4 ± 0.0	916 12.4 ± 0.0	917 20.2 ± 1.7	918 33.3	919 44.3 ± 1.2	920 45.4
927 DE-PT	928 1.6 ± 0.0	929 1.6 ± 0.0	930 3.3 ± 0.2	931 4.7	932 6.1 ± 0.1	933 6.2
940 DE-RU	941 2.4 ± 1.4	942 15.6 ± 0.8	943 8.4 ± 3.0	944 25.2	945 39.0 ± 3.9	946 51.2
954 EN-ES	955 62.8 ± 0.2	956 62.6 ± 0.1	957 113.6 ± 7.6	958 180.0	959 239.4 ± 7.5	960 245.1
969 EN-FI	970 2.6 ± 0.5	971 3.4 ± 0.0	972 5.7 ± 0.2	973 6.1	974 12.2 ± 0.6	975 12.6
984 EN-FR	985 66.8 ± 0.1	986 66.5 ± 0.3	987 92.0 ± 20.2	988 233.1	989 260.1 ± 21.4	990 314.0
999 EN-IT	1000 22.4 ± 0.0	1001 22.3 ± 0.0	1002 39.3 ± 2.9	1003 65.1	1004 87.0 ± 2.8	1005 89.5
1014 EN-NL	1015 34.2 ± 0.1	1016 34.1 ± 0.0	1017 54.3 ± 3.4	1018 84.1	1019 110.3 ± 2.1	1020 111.7
1029 EN-NO	1030 3.0 ± 0.0	1031 2.9 ± 0.0	1032 3.6 ± 0.9	1033 8.6	1034 8.4 ± 0.9	1035 11.8
1044 EN-PL	1045 1.9 ± 0.3	1046 2.2 ± 0.0	1047 4.1 ± 0.1	1048 6.4	1049 8.7 ± 0.3	1050 9.0
1059 EN-PT	1060 2.2 ± 0.2	1061 1.5 ± 0.0	1062 3.1 ± 0.3	1063 4.5	1064 5.6 ± 0.2	1065 5.8
1074 EN-RU	1075 2.7 ± 0.9	1076 13.2 ± 0.6	1077 5.5 ± 2.4	1078 23.8	1079 30.0 ± 5.1	1080 47.8
1089 EN-SV	1090 3.2 ± 0.6	1091 3.3 ± 0.0	1092 4.0 ± 0.7	1093 8.6	1094 8.7 ± 0.9	1095 11.5
1103 ES-FI	1104 3.4 ± 0.5	1105 3.6 ± 0.0	1106 6.2 ± 0.6	1107 9.1	1108 11.9 ± 0.3	1109 12.2
1118 ES-FR	1119 32.3 ± 0.1	1120 32.2 ± 0.1	1121 53.6 ± 4.8	1122 103.1	1123 116.7 ± 7.8	1124 144.0
1138 ES-IT	1139 24.0 ± 0.0	1140 23.9 ± 0.0	1141 41.5 ± 2.9	1142 62.6	1143 83.4 ± 2.0	1144 85.0
1154 ES-NL	1155 28.7 ± 0.0	1156 28.7 ± 0.0	1157 45.7 ± 3.4	1158 73.2	1159 96.5 ± 2.1	1160 97.8
1169 ES-NO	1170 3.4 ± 0.0	1171 3.4 ± 0.0	1172 3.9 ± 0.7	1173 9.1	1174 8.8 ± 0.9	1175 12.4
1184 ES-PT	1185 1.9 ± 0.0	1186 1.5 ± 0.0	1187 3.0 ± 0.2	1188 4.5	1189 6.2 ± 0.1	1190 6.3
1199 ES-RU	1200 3.6 ± 1.2	1201 15.7 ± 0.0	1202 3.7 ± 2.2	1203 25.9	1204 36.3 ± 4.5	1205 50.5
1219 FI-FR	1220 3.6 ± 0.3	1221 6.0 ± 0.3	1222 10.0 ± 0.3	1223 11.2	1224 10.9 ± 0.4	1225 11.2
1234 FI-NO	1235 4.8 ± 0.3	1236 3.5 ± 0.0	1237 6.1 ± 0.5	1238 9.1	1239 11.4 ± 0.5	1240 12.1
1249 FI-PL	1250 2.8 ± 0.0	1251 2.7 ± 0.0	1252 4.8 ± 0.1	1253 7.8	1254 10.3 ± 0.4	1255 10.6
1264 FR-IT	1265 11.6 ± 0.0	1266 11.5 ± 0.0	1267 20.5 ± 1.4	1268 32.6	1269 43.0 ± 0.9	1270 43.7
1279 FR-NL	1280 30.5 ± 0.0	1281 30.5 ± 0.0	1282 49.2 ± 1.0	1283 82.9	1284 111.5 ± 3.9	1285 114.8
1294 FR-NO	1295 3.1 ± 0.4	1296 3.3 ± 0.0	1297 5.3 ± 0.4	1298 8.6	1299 10.5 ± 0.4	1300 11.4
1314 FR-PL	1315 2.4 ± 0.3	1316 2.6 ± 0.0	1317 4.2 ± 1.0	1318 6.8	1319 9.3 ± 0.3	1320 9.5
1329 FR-PT	1330 1.5 ± 0.0	1331 1.5 ± 0.0	1332 2.9 ± 0.1	1333 4.7	1334 6.2 ± 0.1	1335 6.4
1349 FR-RU	1350 1.6 ± 0.5	1351 7.5 ± 0.4	1352 3.9 ± 0.7	1353 12.5	1354 17.8 ± 2.3	1355 25.0
1369 FR-SV	1370 2.9 ± 0.4	1371 3.1 ± 0.0	1372 3.8 ± 1.2	1373 8.5	1374 8.4 ± 0.6	1375 11.4
1389 IT-NL	1390 2.3 ± 0.0	1391 2.3 ± 0.0	1392 4.2 ± 0.2	1393 6.2	1394 8.7 ± 0.2	1395 8.9
1409 IT-PT	1410 1.8 ± 0.0	1411 1.4 ± 0.0	1412 2.9 ± 0.2	1413 4.7	1414 5.8 ± 0.1	1415 5.9
1429 IT-RU	1430 4.2 ± 0.0	1431 16.2 ± 0.0	1432 4.3 ± 1.6	1433 27.2	1434 37.6 ± 5.1	1435 54.4
1449 IT-SV	1450 3.3 ± 0.2	1451 3.3 ± 0.0	1452 4.7 ± 0.9	1453 8.7	1454 9.1 ± 0.9	1455 11.5

901 902 C HYPERPARAMETERS

903 C.1 FINE-TUNING

904
905 We used the Trainer module from Hugging Face’s **transformers** library for fine-tuning. The key
906 hyperparameters and settings were as follows:

- 907 • Optimizer: AdamW
- 908 • Learning rate: 7×10^{-6}
- 909 • Batch size: Automatically determined based on available hardware
- 910 • Early stopping patience: 3 epochs
- 911 • Mixed precision: Enabled (BF16)

912
913 All unspecified settings followed the default values defined in Trainer module.

918
919 Table 2: Time in GPU-hours to recover 99.9% of the optimal hypervolume on held-out datasets,
920 optimizing for three objectives: model size, evaluation loss and BLEU score.

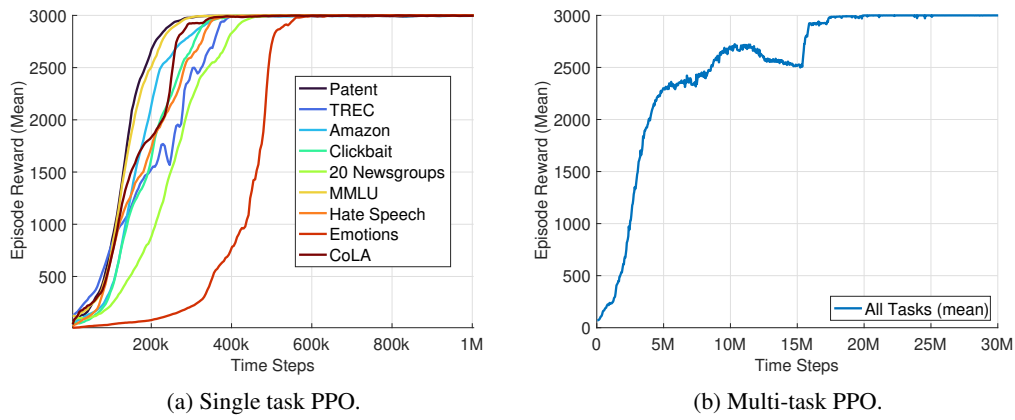
921	Dataset	Oracle	LAMPS (ours)	MO-ASHA	ZigZag	Blind	Exhaustive
922	DE-EN	63.0 \pm 3.7	88.9 \pm 1.1	94.5 \pm 4.5	88.4	120.6 \pm 3.3	123.9
923	DE-ES	30.6 \pm 5.1	51.4 \pm 0.6	49.0 \pm 6.9	53.1	71.4 \pm 2.6	73.6
924	DE-FR	26.0 \pm 2.7	62.7 \pm 3.2	34.5 \pm 5.6	66.1	90.4 \pm 2.8	93.0
925	DE-IT	33.9 \pm 1.9	51.8 \pm 1.1	54.6 \pm 13.3	57.7	76.5 \pm 0.9	77.1
926	DE-NL	29.0 \pm 2.5	32.1 \pm 0.6	44.0 \pm 0.8	45.3	44.9 \pm 0.7	45.4
927	DE-PT	3.7 \pm 0.1	4.2 \pm 0.1	6.2 \pm 0.0	6.2	6.2 \pm 0.1	6.2
928	DE-RU	13.3 \pm 1.4	36.1 \pm 0.1	17.3 \pm 2.4	29.8	49.9 \pm 1.4	51.2
929	EN-ES	62.9 \pm 0.1	94.6 \pm 35.2	99.3 \pm 8.8	180.1	241.7 \pm 4.2	245.1
930	EN-FI	7.3 \pm 0.3	8.3 \pm 0.1	11.9 \pm 0.2	12.6	12.2 \pm 0.3	12.6
931	EN-FR	77.6 \pm 3.1	222.4 \pm 0.0	126.5 \pm 8.9	240.1	309.1 \pm 6.3	314.0
932	EN-IT	23.9 \pm 0.0	62.7 \pm 2.5	39.5 \pm 2.2	65.1	87.0 \pm 2.5	89.5
933	EN-NL	61.4 \pm 3.0	81.9 \pm 1.3	104.0 \pm 4.7	84.1	109.6 \pm 2.2	111.7
934	EN-NO	5.8 \pm 0.4	8.9 \pm 0.5	11.2 \pm 0.1	11.8	11.5 \pm 0.3	11.8
935	EN-PL	4.7 \pm 0.0	5.8 \pm 0.4	8.7 \pm 0.3	9.0	8.7 \pm 0.3	9.0
936	EN-PT	3.2 \pm 0.0	3.6 \pm 0.0	5.3 \pm 1.0	4.5	5.7 \pm 0.1	5.8
937	EN-RU	10.6 \pm 0.1	28.4 \pm 7.4	17.7 \pm 2.9	23.8	46.4 \pm 1.5	47.8
938	EN-SV	5.2 \pm 0.3	7.7 \pm 0.0	11.0 \pm 0.1	11.5	10.2 \pm 0.6	11.5
939	ES-FI	6.8 \pm 0.8	8.8 \pm 0.3	11.6 \pm 0.0	12.2	11.6 \pm 0.4	12.2
940	ES-FR	86.5 \pm 1.2	99.4 \pm 2.0	143.8 \pm 0.0	143.7	142.6 \pm 2.2	144.0
941	ES-IT	43.6 \pm 0.7	59.1 \pm 1.8	81.8 \pm 1.6	64.3	84.4 \pm 0.9	85.0
942	ES-NL	66.5 \pm 2.2	81.9 \pm 4.9	97.7 \pm 0.0	97.7	96.9 \pm 1.3	97.8
943	ES-NO	6.7 \pm 0.7	7.5 \pm 0.3	12.4 \pm 0.0	12.4	11.9 \pm 0.5	12.4
944	ES-PT	3.9 \pm 0.1	3.8 \pm 0.2	6.3 \pm 0.0	6.3	6.3 \pm 0.1	6.3
945	ES-RU	12.5 \pm 3.4	34.5 \pm 1.1	19.0 \pm 0.9	25.9	48.8 \pm 1.4	50.5
946	FI-FR	5.1 \pm 0.0	7.0 \pm 0.5	10.6 \pm 0.1	11.2	10.9 \pm 0.3	11.2
947	FI-NO	8.6 \pm 0.3	8.4 \pm 0.1	12.1 \pm 0.0	12.1	11.9 \pm 0.3	12.1
948	FI-PL	6.6 \pm 0.2	7.1 \pm 0.4	10.6 \pm 0.0	10.6	10.3 \pm 0.4	10.6
949	FR-IT	18.7 \pm 0.0	30.5 \pm 0.3	20.1 \pm 1.5	32.6	42.9 \pm 1.1	43.7
950	FR-NL	74.3 \pm 5.2	80.2 \pm 1.0	114.8 \pm 0.0	114.6	113.9 \pm 1.6	114.8
951	FR-NO	6.2 \pm 0.7	6.7 \pm 0.4	11.4 \pm 0.0	11.4	11.2 \pm 0.2	11.4
952	FR-PL	5.6 \pm 0.2	5.9 \pm 0.0	9.3 \pm 0.2	9.5	9.3 \pm 0.2	9.5
953	FR-PT	3.6 \pm 0.2	4.3 \pm 0.1	6.4 \pm 0.0	6.4	6.3 \pm 0.1	6.4
954	FR-RU	7.3 \pm 0.1	13.3 \pm 3.1	10.8 \pm 0.2	18.6	24.5 \pm 0.7	25.0
955	FR-SV	7.2 \pm 0.4	7.7 \pm 0.1	11.4 \pm 0.0	11.4	11.1 \pm 0.3	11.4
956	IT-NL	6.1 \pm 0.2	6.6 \pm 0.5	8.9 \pm 0.0	8.9	8.8 \pm 0.1	8.9
957	IT-PT	3.8 \pm 0.1	4.2 \pm 0.1	5.7 \pm 0.3	5.9	5.9 \pm 0.0	5.9
958	IT-RU	13.0 \pm 1.5	35.3 \pm 1.8	11.6 \pm 2.7	27.2	50.6 \pm 2.6	54.4
959	IT-SV	6.9 \pm 0.4	7.6 \pm 0.1	11.5 \pm 0.0	11.5	11.2 \pm 0.4	11.5
960							

C.2 PPO

956
957 For the PPO algorithm, we used the implementation from Stable Baselines3 library. The key hyper-
958 parameters and settings were as follows:

- 959 • Learning rate: 1×10^{-4}
- 960 • Minibatch size: 256
- 961 • Num. epochs: 15
- 962 • Discount (γ): 0.99
- 963 • GAE parameter (λ): 0.97
- 964 • Clip range: 0.20
- 965 • VF coeff. c_1 : 0.5
- 966 • Entropy coeff. c_2 : 0.23

967 All policies were trained using the Gymnasium environment API with invalid action masking.

972 **D EMPIRICAL CONVERGENCE ANALYSIS OF THE REWARDS**
973974 In order to provide additional evidence that the reward function defined in equation 7 effectively
975 guides the agent toward the optimal solution set, according to the original multi-objective problem
976 in equation 1, Figure 5 presents a typical reward evolution observed during training, for both single
977 task and multi-task RL (MTRL) using PPO .
978979 For better interpretability and comparison, reward values are normalized such that a value of 3000
980 corresponds to the optimal reward, when the agent exclusively evaluates Pareto-optimal solutions,
981 achieving maximal hypervolume in minimal time. The learned policy exhibits a consistent upward
982 trend in reward, eventually converging to the optimal value.
983996 Figure 5: Normalized reward progression during policy training using PPO algorithm. As expected,
997 multi-task RL takes longer, but it also converges to the optimal reward.
998
9991000 **E DATASETS**
10011003 This section describes the datasets used in our experiments.
10041006 **E.1 TEXT CLASSIFICATION**
10071008 Although the datasets described here correspond to text classification tasks, they cover different NLP
1009 tasks, requiring different linguistic competencies, domain knowledge, and reasoning abilities. This
1010 diversity makes it particularly challenging (and well-suited) for evaluating LAMPS. For datasets
1011 without predefined training and validation splits, we reserve 20% of the data for validation.
10121013 **TREC** A classic question classification benchmark with 6 coarse-grained classes (e.g., abbreviation,
1014 entity, description and abstract concept, human being, location, and numeric value). Task:
1015 Question classification. License: N/A (widely used academic benchmark; originally from UIUC).
10161017 **Clickbait** Contains news headlines labeled as either “clickbait” or “non-clickbait”. Derived from
1018 social media posts (Chakraborty et al., 2016). Task: Binary classification. License: N/A.
10191020 **20 Newsgroups** A collection of 20,000 newsgroup emails across 20 different topics (Lang, 1995).
1021 Task: Topic classification. License: CC BY 4.0.
10221023 **Amazon Reviews (cell-phone)** Subset of the Amazon Product Review 2013 dataset, filtered for
1024 the “Cell Phone reviews” category. Includes star ratings from 1 to 5 and contains 78,930 reviews.
1025 Task: Sentiment classification (5 classes). License: N/A (Amazon public data, widely used in
academia).

1026 **Hate Speech and Offensive Language** A corpus of over 24,000 tweets manually annotated as
 1027 hate speech, offensive but not hateful, or neither (Davidson et al., 2017). Task: Offensive language
 1028 classification (3 classes). License: MIT License.
 1029

1030 **MMLU** Massive Multitask Language Understanding, a benchmark covering 57 diverse subject
 1031 areas from elementary math to law and philosophy. Task: Multi-choice question answering. License:
 1032 MIT License.
 1033

1034 **Patent Classification** Consisting of 35,000 Patent abstracts labeled with Cooperative Patent Clas-
 1035 sification (CPC) codes (9 classes). Task: Topic classification. License: Public domain (based on
 1036 USPTO data).
 1037

1038 **Emotion** A dataset of 20,000 Twitter messages in English annotated with one of six basic emo-
 1039 tions (anger, fear, joy, love, sadness, surprise). Task: Emotion classification. License: MIT License.
 1040

1041 **CoLA** Corpus of Linguistic Acceptability, a dataset of English sentences labeled as grammati-
 1042 cally acceptable or unacceptable. Task: Acceptability classification (binary). License: Unknown
 1043 (academic benchmark from the GLUE suite).
 1044

1045 **SMS Spam** A dataset of SMS messages labeled as spam or ham, widely used in spam detection
 1046 research. Task: Binary classification. License: Open for research use.
 1047

1048 **IMDB** A large-scale movie review corpus containing 50K reviews labeled as positive or negative
 1049 (Maas et al., 2011). Task: Sentiment classification (binary). License: Permissive research license.
 1050

1051 **Financial Phrasebank** A financial-domain sentiment dataset of short sentences annotated by mul-
 1052 tiple experts with high-agreement labels (positive, negative, neutral) (Malo et al., 2014). Task:
 1053 Financial sentiment analysis (3 classes). License: Creative Commons Attribution-NonCommercial-
 1054 ShareAlike 3.0 Unported License.
 1055

E.2 MACHINE TRANSLATION

1057 **OPUS Books** A collection of copyright-free texts translated into multiple languages (Tiedemann,
 1058 2012). License: Available for personal, educational and research use.
 1059

F PRETRAINED LANGUAGE MODELS

1062 Below is the list of pretrained models used during the experiments of this paper:
 1063

F.1 TEXT CLASSIFICATION

1066 **BERT:**

1. google-bert/bert-large-cased-whole-word-masking
2. google-bert/bert-large-uncased-whole-word-masking-fine-tuned-squad
3. google-bert/bert-large-uncased-whole-word-masking
4. google-bert/bert-large-uncased
5. google-bert/bert-large-cased-whole-word-masking-fine-tuned-squad
6. google-bert/bert-large-cased
7. google-bert/bert-base-uncased
8. google-bert/bert-base-multilingual-uncased
9. google-bert/bert-base-multilingual-cased
10. google-bert/bert-base-german-dbmdz-uncased
11. google-bert/bert-base-german-dbmdz-cased
12. google-bert/bert-base-german-cased
13. google-bert/bert-base-chinese
14. google-bert/bert-base-cased

1080 **GPT:**

1081

1082 1. openai-community/gpt2

1083 2. openai-community/gpt2-medium

1084 3. openai-community/gpt2-large

1085 4. openai-community/gpt2-xl

1086

1087 **RoBERTa:**

1088

1089 1. FacebookAI/roberta-base

1090 2. FacebookAI/roberta-large

1091 3. FacebookAI/xlm-roberta-base

1092 4. FacebookAI/xlm-roberta-large

1093 5. FacebookAI/xlm-roberta-large-fine-tuned-conll02-dutch

1094 6. FacebookAI/xlm-roberta-large-fine-tuned-conll02-spanish

1095 7. FacebookAI/xlm-roberta-large-fine-tuned-conll03-english

1096 8. FacebookAI/xlm-roberta-large-fine-tuned-conll03-german

1097

1098 **OPT:**

1099

1100 1. facebook/opt-125m

1101 2. facebook/opt-350m

1102 3. facebook/opt-1.3b

1103 4. facebook/opt-2.7b

1104 5. facebook/opt-6.7b

1105

1106 **Llama:**

1107

1108 1. meta-llama/Llama-3.2-1B

1109 2. meta-llama/Llama-3.2-1B-Instruct

1110 3. meta-llama/Llama-3.2-3B

1111 4. meta-llama/Llama-3.1-8B

1112

1113 **DistilBERT:**

1114

1115 1. distilbert/distilbert-base-multilingual-cased

1116 2. distilbert/distilbert-base-german-cased

1117 3. distilbert/distilbert-base-uncased-distilled-squad

1118 4. distilbert/distilbert-base-cased-distilled-squad

1119 5. distilbert/distilbert-base-cased

1120 6. distilbert/distilbert-base-uncased

1121 7. distilbert/distilroberta-base

1122 8. distilbert/distilgpt2

1123

1124 **ALBERT:**

1125

1126 1. albert/albert-xlarge-v2

1127 2. albert/albert-xxlarge-v2

1128 3. albert/albert-xxlarge-v1

1129 4. albert/albert-xlarge-v1

1130 5. albert/albert-large-v2

1131 6. albert/albert-large-v1

1132 7. albert/albert-base-v2

1133 8. albert/albert-base-v1

1134

1135 **LUKE:**

1136

1137 1. studio-ousia/mluke-large

1138 2. studio-ousia/mluke-large-lite

1134 3. studio-ousia/mluke-base-lite
 1135 4. studio-ousia/mluke-base
 1136 5. studio-ousia/luke-japanese-base
 1137 6. studio-ousia/luke-japanese-base-lite
 1138 7. studio-ousia/luke-japanese-large-lite
 1139 8. studio-ousia/luke-japanese-large
 1140 9. studio-ousia/luke-large-lite
 1141 10. studio-ousia/luke-base-lite
 1142 11. studio-ousia/luke-large
 1143 12. studio-ousia/luke-base

1144 **DeepSeek:**

1145 1. deepseek-ai/DeepSeek-R1-Distill-Qwen-1.5B
 1146 2. deepseek-ai/DeepSeek-R1-Distill-Qwen-7B
 1147 3. deepseek-ai/DeepSeek-R1-Distill-Llama-8B

1149 **Qwen:**

1150 1. Qwen/Qwen2.5-0.5B
 1151 2. Qwen/Qwen2.5-1.5B
 1152 3. Qwen/Qwen2.5-3B
 1153 4. Qwen/Qwen2.5-7B

1156 **F.2 MACHINE TRANSLATION**

1158 **Helsinki-NLP:**

1159 1. Helsinki-NLP/opus-mt-en-sv
 1160 2. Helsinki-NLP/opus-mt-tc-bible-big-deu_eng_fra_por_spa-mul

1162 **_mBART:**

1163 1. facebook/mbart-large-50
 1164 2. facebook/mbart-large-50-many-to-many-mmmt
 1165 3. facebook/mbart-large-50-many-to-one-mmmt
 1166 4. facebook/mbart-large-50-one-to-many-mmmt
 1167 5. facebook/mbart-large-cc25
 1168 6. facebook/mbart-large-en-ro

1170 **T5:**

1171 1. google/t5/t5-3b
 1172 2. google/t5/t5-base
 1173 3. google/t5/t5-large
 1174 4. google/t5/t5-small
 1175 5. google/long-t5-local-large
 1176 6. google/long-t5-tglobal-xl

1178 **mT5:**

1179 1. google/mt5-base
 1180 2. google/mt5-large
 1181 3. google/mt5-small
 1182 4. google/mt5-xl

1184 **UMT5:**

1186 1. google/umt5-base
 1187 2. google/umt5-small

1188 **G ADDING NEW MODELS TO THE META-DATASET**
1189

1190 To incorporate a new model into the recommendation pool of LAMPS, it must first be integrated
1191 into the meta-dataset. We refer to this process as *model fingerprinting*. Because LAMPS relies on
1192 meta-learning, it is necessary to observe the actual performance of the new model on known datasets
1193 before the system can generalize its behavior to unseen datasets. This integration requires two steps:
1194

1195 1. The new LLM must be fine-tuned on all datasets currently included in the meta-dataset,
1196 with all relevant metrics recorded.
1197 2. The reinforcement learning policy must be retrained on the expanded meta-dataset.
1198

1199 Currently, complete retraining is the recommended procedure for reliable integration of new models.
1200 Although incremental training strategies could further reduce the computational overhead, the cost
1201 of full retraining is already negligible compared to the fine-tuning runs required to expand the meta-
1202 dataset.

1203 The ideal number and diversity of datasets in the meta-dataset remains an open research question.
1204 A smaller set of datasets facilitates the addition of new models, since each integration requires
1205 fewer fine-tuning runs. Conversely, a larger and more diverse collection typically improves the
1206 generalization ability of the learned policy to unseen tasks. How to balance these competing goals
1207 remains an open challenge for future work.

1208
1209 **H PROOF OF THEOREM 1**
1210

1211 *Proof.* We first prove that the maximizer $X_\lambda = \arg \max_{X \subset \mathcal{X}} H_{\mathcal{D}}(X, r) - \lambda|X|$ is a subset of Pareto
1212 solutions X^* , that is, for any $\lambda > 0$, $X_\lambda \subset X^*$. This is proved by contradiction. Suppose that there
1213 exists a $x \in X_\lambda$ that is not Pareto-optimal. Then, there exists a $x^* \in \mathcal{X}$ dominating x such that
1214 $\Lambda([x, r]) < \Lambda([x^*, r])$ holds. Denote X_λ^* the set obtained from X_λ by replacing x with x^* . By the
1215 definition of $H_{\mathcal{D}}$, we know $H_{\mathcal{D}}(X_\lambda, r) < H_{\mathcal{D}}(X_\lambda^*, r)$. Then, it holds

1216
$$H_{\mathcal{D}}(X_\lambda, r) - \lambda|X_\lambda| = H_{\mathcal{D}}(X_\lambda, r) - \lambda|X_\lambda^*| < H_{\mathcal{D}}(X_\lambda^*, r) - \lambda|X_\lambda^*|.$$

1217

1218 This contradicts the assumption that X_λ is the maximizer of problem (3). Hence, for any $\lambda > 0$, we
1219 know $X_\lambda \subset X^*$. Below we prove the *if* part and the *only if* part respectively. **The if part:** In this
1220 part, we prove that if equation 4 holds, then the optimal solution $X^* \subset \mathcal{X}$ of problem equation 3 con-
1221 tains only and exactly all Pareto-optimal solutions. Let $X_\lambda = \arg \max_{X \subset \mathcal{X}} H_{\mathcal{D}}(X, r) - \lambda|X|$. From
1222 the above discussion we know $X_\lambda \subset X^*$. Suppose $|X^*| - |X_\lambda| = s$. We denote $\{x_{i_1}, \dots, x_{i_s}\} \subset$
1223 X^* the subset of X^* such that $\{x_{i_1}, \dots, x_{i_s}\} \cap X_\lambda = \emptyset$. We define $X_k = X_\lambda \cup \{x_{i_1}, \dots, x_{i_k}\}$
1224 for all $k \in \{0, 1, \dots, s\}$. Then, we know $X_s = X^*$, $X_0 = X_\lambda$ and $|X_{k+1}| - |X_k| = 1$ for all
1225 $k \in \{0, 1, \dots, s-1\}$. Note that

1226
$$\begin{aligned} & H_{\mathcal{D}}(X^*, r) - \lambda|X^*| - (H_{\mathcal{D}}(X_\lambda, r) - \lambda|X_\lambda|) \\ &= H_{\mathcal{D}}(X^*, r) - H_{\mathcal{D}}(X_\lambda, r) - \lambda(|X^*| - |X_\lambda|) \\ &= H_{\mathcal{D}}(X_s, r) - H_{\mathcal{D}}(X_0, r) - s\lambda \\ &= \sum_{k=1}^s (H_{\mathcal{D}}(X_k, r) - H_{\mathcal{D}}(X_{k-1}, r) - \lambda) \\ &\geq \sum_{k=1}^s \left(H_{\mathcal{D}}(X_k, r) - H_{\mathcal{D}}(X_{k-1}, r) - \min_{x \in X, X \subset X^*} \Delta H_{\mathcal{D}}(x|X) \right) \\ &\geq 0, \end{aligned} \tag{8}$$

1237 where the last second inequality used equation 4 and the last inequality used the definition of
1238 $\min_{x \in X, X \subset X^*} \Delta H_{\mathcal{D}}(x|X)$. **The only if part:** To prove this part of the result, we only need
1239 to show that there exists an optimization problem whose Pareto solution set X^* with $|X^*| = s$
1240 satisfies that for any sequence of subsets $\{X_i\}_{i=1}^s$ satisfying $X_i \subset X^*$ and $|X_i| = i$, it holds

1241
$$\max_{i \in \{2, \dots, s\}} H_{\mathcal{D}}(X_i, r) - H_{\mathcal{D}}(X_{i-1}, r) = \min_{x \in X, X \subset X^*} \Delta H_{\mathcal{D}}(x|X). \tag{9}$$

1242 On the other hand, from equation 8 and the definition of X^* we know
 1243

$$1244 H_{\mathcal{D}}(X^*, r) - \lambda|X^*| - (H_{\mathcal{D}}(X_{\lambda}, r) - \lambda|X_{\lambda}|) = \sum_{k=1}^s (H_{\mathcal{D}}(X_k, r) - H_{\mathcal{D}}(X_{k-1}, r)) - s\lambda \geq 0.$$

1247 Hence, we have $\sum_{k=1}^s (H_{\mathcal{D}}(X_k, r) - H_{\mathcal{D}}(X_{k-1}, r)) \geq s\lambda$. Combining this observation with
 1248 equation 9 together, we get

$$1249 \min_{x \in X, X \subset X^*} \Delta H_{\mathcal{D}}(x|X) \geq \lambda.$$

1250 The proof is completed by noting that equation 9 always holds for arbitrary X^* with $|X^*| = 2$. \square
 1251

1253 I THE USE OF LARGE LANGUAGE MODELS (LLMs)

1255 We used large language models solely for surface-level editing: spelling and grammar correction,
 1256 and minor wording improvements. LLMs were *not* used for idea generation, experiment design,
 1257 data analysis, coding, mathematical derivations, or substantive content creation.

1258
 1259
 1260
 1261
 1262
 1263
 1264
 1265
 1266
 1267
 1268
 1269
 1270
 1271
 1272
 1273
 1274
 1275
 1276
 1277
 1278
 1279
 1280
 1281
 1282
 1283
 1284
 1285
 1286
 1287
 1288
 1289
 1290
 1291
 1292
 1293
 1294
 1295